Spectral subtraction and enhancement for torsional waves propagating in coated pipes

Wenbo Duan[1*]; Jamil Kanfoud[1]; Matthew Deere[2]; Peter Mudge[2]; Tat-Hean Gan[1,2*]

1 Brunel Innovation Centre, Brunel University London, Uxbridge, Middlesex, UK, UB8 3PH

2 Integrity Management Group, TWI Ltd, Cambridge, UK, CB21 6AL

Wenbo.Duan@brunel.ac.uk

Tat-Hean.Gan@brunel.ac.uk

Abstract

Ultrasonic guided waves are routinely used for inspection of pipelines. The technique is well established for uncoated pipes where attenuation is very low. However, when the pipe is coated, buried or immersed, sound energy will be absorbed by the coating or radiate into the surrounding medium. Attenuation will increase and the scanning distance will be significantly reduced. The noise level can also increase when the condition of the coating material degrades with age and the bonding condition between pipe and coating becomes unevenly distributed. The increase of attenuation ratio and noise level therefore makes the inspection of ultrasonic waves propagating in coated and buried pipelines particularly difficult. It is often desirable to identify small features amongst the noise floor. To improve signal to noise ratio under these conditions, two techniques are proposed for the study of the propagation of torsional waves in Denso Tape coated pipes. A frequency domain, backward wave cancelling algorithm is used

to eliminate the reflected waves coming from the backward direction and clean up the signal. On this basis, a spectral subtraction method is used, which requires knowledge of a small section of pipe that includes no real features, so that the signal from this region provides the characteristic noise signature of the pipe itself. The spectrum of the noise signature is calculated and then subtracted from the total signal using a sliding window technique. Furthermore, a signal region, for instance，the reflected signal from a pipe weld or end, is specified. This represents the characteristic of the incident signal and any signal similar in shape will be enhanced using the sliding window technique. These two techniques serve to reduce the noise floor and enhance small signals that may be buried in it. This is important for ultrasonic non-destructive testing applications in coated and buried pipes.

Key words: Guided waves; Denso Tape coated pipe; Backward wave cancelling; Spectral subtraction; Spectral enhancement.

I. Introduction

Ultrasonic guided waves are routinely used for non-destructive inspection of pipelines. This is normally based on a pulse-echo principle, and the technique is highly successful for pipelines that are uncoated and unburied, so that attenuation is low [1-4]. Recently, the technique has been advanced to address problems in more challenging conditions, such as coated and/or buried pipelines. The coating material is normally viscoelastic, and absorbs sound energy while for buried pipelines, sound energy can leak into the surrounding medium. In both cases, attenuation of guided waves is high in the conventional long range ultrasonic testing frequency range from 20kHz to 100kHz and the effective scanning distance of guided waves is thus significantly reduced.

Furthermore, in addition to the reduction in signal strength, the noise level can also increase, especially for coating materials that have been present for a number of years. In this case, bonding conditions between the coating material and the pipe substrate become uneven due to pressure changes and temperature variations around the pipe, etc., and noise signals are created. It is thus often necessary to identify small signals that may be beneath the noise floor and signal interpretation is very challenging, because of the randomness of the noise signature. This article studies the propagation of torsional waves in a pipe coated with Denso Tape, wrapped evenly onto the pipe by a wrapping machine. The maximum coating length studied here was 5.5m, and it can already be seen at this length that the reflected signal from a pipe feature (weld) is lower than the amplitude of some noise peaks. A spectral subtraction and enhancement algorithm is proposed to improve signal to noise ratio. A sliding Hanning window is used to remove the noise spectrum and enhance the signal spectrum segment by segment. The signal is then reconstructed through inverse Fourier transformation and combination of segments.

The attenuation of guided axisymmetric elastic waves in Bitumen coated pipes has been studied by Kirby et al [5, 6] who present a hybrid finite element model to study the scattering of torsional and longitudinal waves from axisymmetric defects in coated pipes. The material properties of Bitumen are extracted by comparing theoretical predictions with experimental measurements for two different incident modes over a large frequency range. Kuo and Suh have proposed an analytical model to study propagation of longitudinal waves in a multi-layer coated pipe [7]. The influence of multi-layer viscoelastic coating materials on wave dispersion and attenuation is investigated. Leinov et al have studied the attenuation of axisymmetric elastic waves in pipes that are coated and buried [8, 9]. They found that low impedance (product of

density and the real part of the shear velocity) coating materials could trap sound energy inside the pipe so that little energy leaks into the surrounding medium. Duan et al presented an efficient one dimensional numerical model to study wave propagation in coated and buried pipes [10]. A new stretching function is proposed to allow the model to converge quickly even with a thin, perfectly matched layer (PML). A similar sound isolation effect could be observed for coating material with impedance larger than that of the surrounding medium. However, this isolation may occur at a higher frequency range. An extensive list of reference papers can be found in the literature which are related to guided wave propagation in coated and/or buried pipes [11-20].

Benmeddour et al [21] and Duan et al [22, 23] presented a hybrid, finite element model to study wave scattering from a non-axisymmetric defect in a solid cylinder, uncoated pipe and coated pipe, respectively. A small section of the waveguide is meshed which ensured that the model could be executed quickly. The modal amplitude of scattered flexural modes is presented, in addition to the usual axisymmetric modes. Duan et al [24] further presented a numerical model to study scattering of torsional waves from an axisymmetric defect in a buried pipe. The perfectly matched layer method is used to close the problem both in the central finite element section and in the uniform modal expansion region. Sun et al [25] studied the mode conversion behaviour of Lamb and shear-horizontal waves in a plate to longitudinal and torsional guided waves in a pipe. EMAT transducers were developed to produce waves in the plate. The plate was then wrapped onto the pipe in two different waves, which facilitated the study of different mode conversion behaviour. A number of other analytical and numerical techniques have been proposed to study wave scattering from discontinuities in waveguides [26-31].

These references investigate the physics of the problem. The length of the coated and/or buried section in the experimental measurements [5-6, 8-9] was very small, usually less than 2m, so that the reflected signal from a defect or pipe end could be identified clearly. In practical non-destructive testing applications on coated pipe, a small section of the coating is removed to allow the ultrasonic transducers to be mounted onto the wall. If the pipe is buried, then excavation work is required to allow access. It is thus desirable to scan the longest possible pipe section in a single pass. In this case, the reflected signal from a pipe feature can be lower than the noise floor, and interpretation of the signal is challenging. To clean up the signal, a common practice is to sum and average the signals received from all the transducers in each ring. This then delivers the axisymmetric modes. However, because of the differences between transducers, coherent noise can appear, in addition to other environmental and electric noise.

Furthermore, the signal can also be reflected several times between different features when interpretation of the signal could be improved by cancelling reflected waves coming from the backward direction. Kemp et al proposed a time domain algorithm to separate forward and backward acoustic waves using multiple microphones [32]. Two calibration runs were carried out to measure the time domain transfer functions for each pair of microphones. The loudspeaker and calibration tube are also interchanged between these measurements to allow calculation of forward and backward transfer functions. This arrangement is difficult in an industrial context, so that Groves and Lennox proposed a method to simplify the calibration procedure [33]. A source tube run out is used to increase the length of the signal. This allowed forward travelling waves to be windowed out and thus forward inter-microphone transfer functions to be measured. The backward transfer functions are then calculated by reversing the forward travelling waves. Groves and Lennox [33] also tested another wave separation

algorithm which significantly simplifies the calibration procedure; however, the result may include/generate more low frequency interference. These algorithms are proposed for acoustic waves propagating in air, and the loudspeaker and microphones are separated using a source tube. For elastic waves, the same transducers used to generate the waves are used to receive them, so that modifications are required and the transfer functions have to be measured in a different way, reported in section III of this paper.

The wave separation techniques are only used to separate forward and backward propagating waves. They can reduce the number of pulses and simplify the interpretation of signals, however, they cannot improve signal to noise ratio. When the amplitude of the reflected signal is lower than the noise level, additional signal processing algorithms are required. Currently, there is no well-established method for improving signal to noise ratio for guided waves propagating in coated and/or buried pipes. The major difficulty is that the piezoelectric and coherent noise is coming from differences between transducers. This type of noise is associated with high order flexural modes which are also dispersive [22, 23]. The wave modes of coherent noise are unknown and highly problem dependent, thus making them difficult to remove. In speech analysis, a spectral subtraction algorithm is widely used to reduce acoustically added noise [34-40]. This suppresses stationary noise relative to speech by subtracting the spectral noise bias calculated during non-speech activity. A sliding window is used to remove noise, segment by segment. This algorithm requires the noise spectrum to be estimated accurately. If the noise estimate is not perfect, then remnant noise will appear. The remnant noise is distracting to humans and causes hearing fatigue. A number of variations have been proposed based on this algorithm. Upadhyay and Karmakar presented a comparison and simulation study of different forms of subtraction-type

algorithms [40]. The task is to produce more pleasant speech with minimal remnant noise.

In this article, the spectral subtraction algorithm is used to remove noise associated with the torsional wave T(0,1) propagating in coated pipes. This is important for non-destructive inspection of coated pipes when the guided wave signal becomes comparable to the noise because of its high attenuation due to the coating. Denso Tape material is used here, and material properties of the coating have been studied theoretically and experimentally by Duan et al [41]. The focus is to clean up the signal by removing travelling components of the torsional wave mode reflected from the backward direction and improving signal to noise ratio. The frequency domain wave separation algorithm is used, and the transfer functions between two rings of transducers are calculated by the reflected signals from welds and pipe ends. The spectral subtraction method is used to remove environmental, piezoelectric and coherent noise. The coherent noise could be a mode converted signal from the T(0,1) mode, and is thus related to T(0,1) which means that it is not possible to remove all the coherent noise using the spectral subtraction method. A spectral enhancement technique is proposed in which the windowed signal is enhanced if there is a high similarity between the signal and a T(0,1) mode. The structure of the paper is as follows. The introduction is presented in section I. The experimental procedure is given in section II, and the signal processing algorithm is presented in section III. The results and discussions are presented in section IV. Finally, conclusions are drawn in section V.

II. Experiments

A standard pipe segment is 6m long, and pipelines are constructed by welding these segments together. It is thus common to see a series of welds regularly spaced in a long pipe run. A typical 18.55m long, 8inch schedule 40 pipe is shown in Fig. 1. The pipe was partially covered by Denso Tape coating. A standard wrapping machine (Denso 250-1200, Winn & Coales Ltd.) was used to wrap the coating evenly onto the pipe. The length of the coating was gradually increased from 1m to 5.5m. The pipeline was supported by three pipe supports with insulation foam placed between them and the pipeline to prevent them scattering any elastic waves.

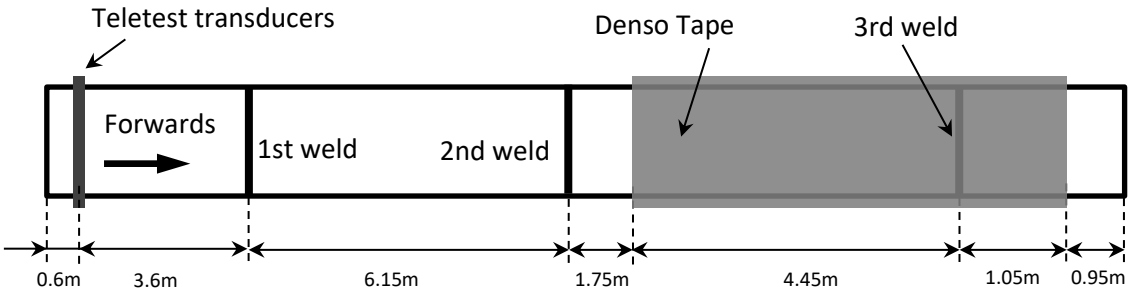

Fig. 1 Structure of the test-rig

A Teletest MK 4 system was used to generate a transient 10-cycle, Hanning-windowed T(0,1) wave mode. The Teletest MK 4 has two rings of transducers separated axially by 30cm. Each ring has 24 transducers equally spaced around the circumference of the pipe. A phase delay was applied between the two rings so that the incident torsional wave was generated in the forward direction (marked in Fig. 1) only. In practice a little bit of signal could still leak into the backward direction, because the transducers are slightly different and themselves generate slightly different phase delays. These

transducers were also used to receive the torsional waves reflected from welds and pipe ends, etc. To eliminate the influence of higher order flexural modes, the signals received by all the transducers in each ring were summed and then averaged. For each ring, an averaged signal as a function of time was produced. The waves will be further reflected back and forth between pipe ends and welds. The measured reflected signal from different features on the pipe is shown in Fig. 2. The centre frequency of the pulse is 40kHz. The torsional wave speed is 3260 m/s. Multiplication of wave speed and travel time gives the travel distance of each signal. Since a pulse-echo principle is used, where the signal travels to a feature and returns, this travel distance is divided by two to give the distance from the feature to the tool. This is shown on the horizontal axis of Fig. 2.

In Fig. 2, the features are labelled by comparing the measured distance to the actual distance shown in Fig. 1. Note that the pulses can be multiply reflected between welds and pipe ends, and so a number of 'repeated' signals appear in Fig. 2. The 'repeated n^{th} weld' in Fig. 2 means that the signal has been reflected by the n^{th} weld and other features, thus representing a number of 'repeated' pulses associated with the weld. This makes the interpretation of the signal difficult, as the number of pulses is much larger than the number of features on the pipe. Furthermore, the incident pulse is assumed to propagate in the forward direction only, while some incident signal could still leak into the backward direction. The leaked signal will then be reflected by the pipe near end and welds, etc, and is clearly visible in Fig. 2. In this case, it is possible for the repeated signal to be larger than the first reflected signal from the 1^{st} or 2^{nd} weld, due to the overlaying of double reflections from the leaked signal and the forward propagating incident signal. The detailed wave path analysis will be given in section IV of this paper.

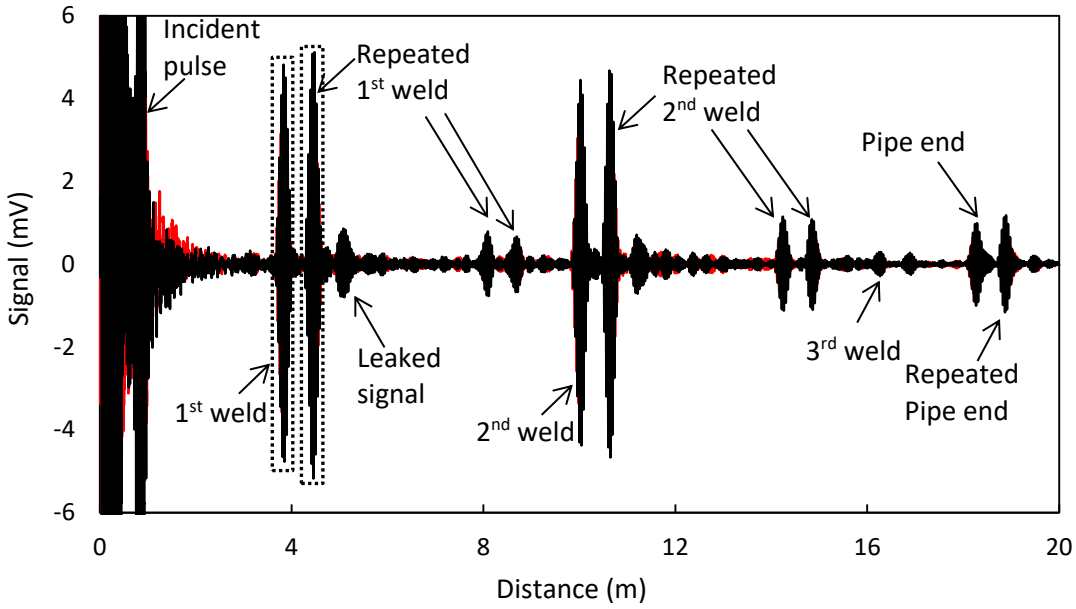

Fig. 2 Original received signal for a 40kHz centre frequency T(0,1) pulse incident on pipe coated with 5.5m Denso Tape. ——, ring a; ——, ring b.

III. Signal processing technique

Two rings of transducers were used to receive signals reflected back from different pipe features. In this paper, the signals received by the first and second rings are denoted by $p_a(t)$ and $p_b(t)$, respectively. The ring set-up is shown in Fig. 3. The corresponding frequency spectra are denoted by $P_a(\omega)$ and $P_b(\omega)$. A frequency-domain, wave separation algorithm can be used to calculate the reflected echoes of the torsional T(0,1) wave mode coming from the forward direction [32]:

$$P_b^-(\omega) = \frac{H_{ab}(\omega) \cdot P_a(\omega) - H_{ab}(\omega)H_{ba}(\omega) \cdot P_b(\omega)}{1 - H_{ab}(\omega) \cdot H_{ba}(\omega)} \quad (1)$$

Here, H_{ab} is the Fourier transform of the windowed time domain transfer function from ring a to ring b, and H_{ba} is the corresponding transfer function from ring b to ring a. Note that a pulse echo principle is used to identify the locations of features on the pipe, and so P_b^- is used to calculate returned echoes from features located in the forward direction (see Fig. 3). The reflected echoes from features located in the backward direction are eliminated. No additional measurements are required to calculate the transfer functions between the two rings: the reflections from the pipe welds and pipe ends can themselves be used to calculate the transfer functions. This normalisation procedure is detailed in the next section. The inverse Fourier transform of $P_b^-(\omega)$ gives the time domain backward propagating wave $p_b^-(t)$ as:

$$p_b^-(t) = \frac{1}{2\pi}\int_{-\infty}^{\infty} P_b^-(\omega)\, e^{i\omega t} d\omega \tag{2}$$

$\mathrm{p_b^-(t)}$ contains both signal and noise. The signal is coming from a short Hanning-windowed incident pulse and the incident signal is further scattered by features on the pipe. The noise could be piezoelectric noise, coherent noise, pipeline noise and environmental noise. As a result, signal and noise will normally change with time. To eliminate noise and enhance signal, it is desirable to work on segments of $\mathrm{p_b^-(t)}$, where short time pulses can be separated from each other. A Hanning window is thus multiplied with $\mathrm{p_b^-(t)}$, and further spectral techniques are applied to each segment of $\mathrm{p_b^-(t)}$. The window then slides through the entire duration of $\mathrm{p_b^-(t)}$, and all the segments are then weighted and summed. The weighting of each segment depends on the ratio of the area of overlap between adjacent sliding windows to the individual window length. This ensures the signal processing technique covers the whole duration of $\mathrm{p_b^-(t)}$.

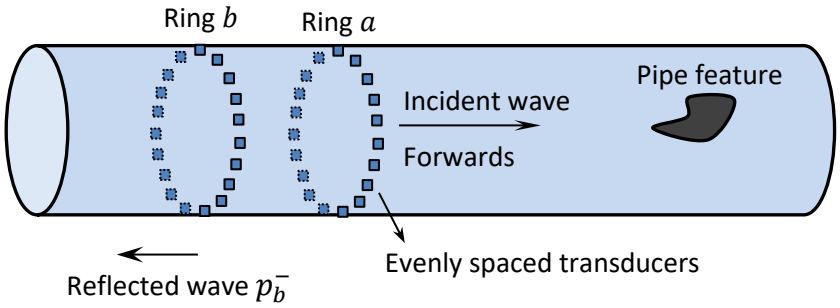

Fig. 3 Ring set-up diagram and direction of separated wave p_b^- reflected from pipe features located in the forward direction.

The structure of the sliding Hanning window is shown in Fig. 4. The length of the window is related to the duration of the scattered signals. For ultrasonic non-destructive testing, it is a normal practice to use 10 cycled Hanning-windowed incident pulses. In this case, the length of the sliding window shall be smaller than the length of the incident pulse, because the edges of the scattered pulses are normally coloured by noise. Furthermore, a small offset between two adjacent windows is set to ensure that the scattered signals can be captured by the sliding window and are as close to the centre of the window as possible due to the large normalisation amplitude there.

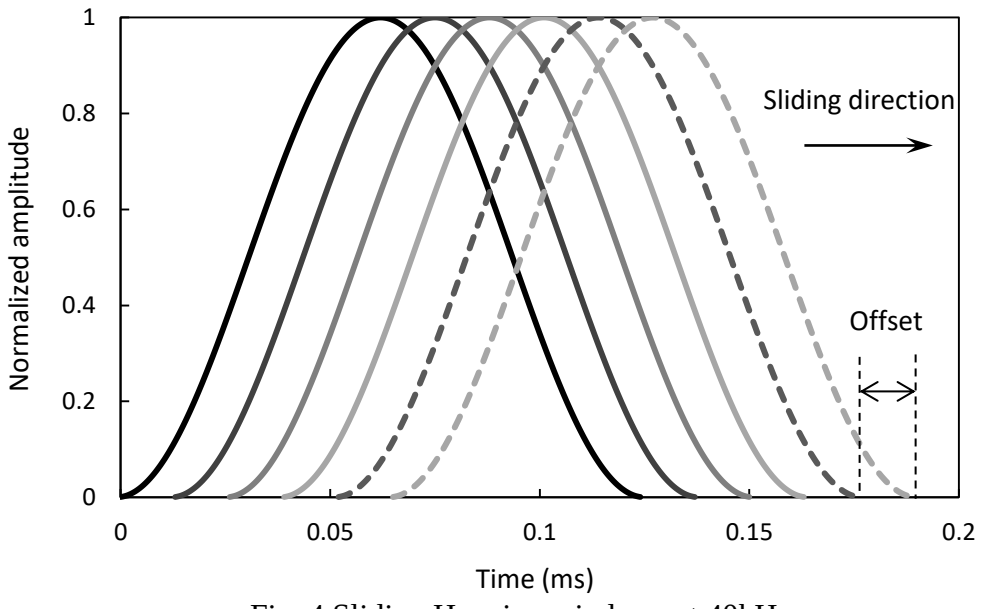

Fig. 4 Sliding Hanning windows at 40kHz.

Each segment of $p_b^-(t)$ can be obtained by a weighting of the Hanning window as:

$$y_n(t) = p_b^-(t) * \mathrm{hann}(t) \tag{3}$$

Here, $\mathrm{hann}(t)$ is the nth sliding Hanning window shown in Fig. 4, and $y_n(t)$ is the nth segment of $p_b^-(t)$.

$y_n(t)$ can be represented as:

$$y_n(t) = s(t) + \mathrm{n}(t) \tag{4}$$

Here, $\mathrm{s}(\mathrm{t})$ represents true scattered signals from the features on the pipe, whereas $\mathrm{n}(\mathrm{t})$ represents noise. It is assumed that the noise is uncorrelated to the T(0,1) signal, so that the power spectrum has no cross-terms [40]:

$$|Y(\omega)|^2 = |S(\omega)|^2 + |\mathrm{N}(\omega)|^2 \tag{5}$$

$Y(\omega)$ is a complex number at each frequency where the amplitude is represented as $|Y(\omega)|$, and the phase is represented as $\theta(\omega)$. To reconstruct the true signal $S(\omega)$ from Eq. (5), it is necessary to know the signature of the noise, $\mathrm{N}(\omega)$. This can be done by manually selecting a small region from $p_b^-(t)$ that contains only noise. The noise signature can be obtained by Fourier transforming and then averaging the noise spectrum. The absolute amplitude of the estimated noise signature is denoted as $\left|\widetilde{\mathrm{N}}(\omega)\right|$. Its phase is of no importance here and is disregarded. The spectrum of the scattered signal can be reconstructed as:

$$\tilde{S}(\omega) = \sqrt{\left[|Y(\omega)|^2 - \left|\widetilde{\mathrm{N}}(\omega)\right|^2\right]}\, e^{i\theta(\omega)} \tag{6}$$

Here, the phase of the reconstructed signal is assumed to be the same as the phase of the original signal, $Y(\omega)$. This avoids the shift of the pulse signal in the time domain. However, the amplitude of the noise signature has been removed. Taking the inverse Fourier transform of Eq. (6), and adding the segments gives the time domain signal as:

$$\tilde{s}(t) = \sum \alpha * ifft\left[\tilde{S}(\omega)\right] \tag{7}$$

Here, a weighting coefficient α is applied to each segment, because of the overlap between windows shown in Fig. 4. The coefficient α equals the ratio between the offset and the width of the sliding Hanning window (see Fig. 4).

Eq. (6) removes the noise signature from the original signal. Here, the noise signature is assumed to remain constant throughout the time domain. However, this is not always the case for guided waves propagating in pipes, where coherent noise can appear in different areas, and their spectra will be different in different segments. To further enhance the scattered T(0,1) mode, the same sliding window technique Eq. (3) could be applied to $\tilde{s}(t)$. The new segment can be denoted as $z_n(t)$, and the Fourier transform of the signal gives $Z(\omega)$. The task is to determine if $z_n(t)$ is T(0,1). This can be done by comparing $Z(\omega)$ with the spectrum of a windowed pulse reflected from a weld. (since there are regular welds associated with a pipeline and it is easy to identify at least one). The spectrum of the weld signal is denoted as $T(\omega)$, and is a baseline T(0,1) mode. Both the segment signal $Z(\omega)$ and the weld signal $T(\omega)$ are normalised so that the amplitude at the centre frequency of the incident pulse is one. The similarity between $Z(\omega)$ and $T(\omega)$ can be determined by comparing the root-mean-square of their difference:

$$d_s = \text{rms}[Z(\omega) - T(\omega)] \tag{8}$$

If d_s is close to zero, then $Z(\omega)$ is similar to $T(\omega)$ and $z_n(t)$ can be considered a T(0,1) mode. In practice, there will always be some differences between spectra of signals reflected from different features, and to avoid missing a true signal from a different feature, a threshold value is set to d_s. This is to say, $z_n(t)$ will be considered as a T(0,1) mode if d_s is smaller than the threshold value. The choice of this threshold value will be discussed in the next section. In this case, the amplitude of $Z(\omega)$ will be increased by 40dB and the phase of $Z(\omega)$ remains the same, i.e.,

$$\tilde{Z}(\omega) = 100|Z(\omega)|e^{i\theta(\omega)} \tag{9}$$

The time domain signal $\tilde{z}(t)$ can be reconstructed by applying an inverse Fourier transformation, i.e., Eq. (7) to $\tilde{Z}(\omega)$. Note that the spectrum $T(\omega)$ is defect dependent. For a non-axisymmetric defect, the spectrum of the defect signal may be very different to the spectrum of the weld signal, and identification of the defect signal will be more challenging. In this case, the spectral subtraction method is still working, however, the spectral enhancement method would require further work on the classification of feature signals.

IV. Results and Discussion

To reduce the number of repeated pulses shown in Fig. 2, the wave cancelling algorithm of Eq. (1) can be used. This requires the transfer functions between the two rings of transducers to be calculated. For acoustic pulse reflectometry applications, a usual practice is to use an additional calibration tube, and interchange positions of the

loudspeaker and the calibration tube. However, for ultrasonic guided wave propagation problems, the installation of an additional calibration tube is not an option because the transducers used to generate ultrasonic waves are also used to receive waves. Furthermore, if the position of the Teletest transducers is changed, then the coupling between the tool and the pipe wall will also be changed, and this would change the transducer transmitting and receiving characteristics. It is preferable to keep the position of the tool fixed while calculating the transfer functions of the two rings. A convenient way to do this is to use existing axisymmetric features on the pipe, for instance, welds and pipe ends etc. In Fig. 2, two pulses are windowed which can be used to calculate the transfer functions of the two rings.

A zoomed-in view of these two pulses is shown in Fig. 5. Note that the main incident wave is generated in the forward direction (see Fig. 3), and the interest is in the forward direction, so that any wave coming from the backward direction is of no interest. The first windowed pulse from Fig. 2 is used to calculate the transfer function from ring a to ring b, and the second windowed pulse is used to calculate the transfer function from ring b to ring a. The wave paths for these two pulses are shown in Figs. 5(a) and (b). In Fig. 5(a), the pulse is reflected from the 1st weld only. This pulse then passes the tool, and is reflected by the near pipe end. The pulse will then travel in the forward direction and will be received by the tool again, as shown in Fig. 5(b). The second pulse is slightly larger than the first, because the second pulse represents the overlaying of two pulses. The leaked signal will be reflected by the near pipe end and then by the 1st weld, and arrive at the tool at exactly the same time. The paths of these two pulses starting in opposite directions are shown in Fig. 5(b), and it can be seen that their travel distances are equal. This means that the transfer function from ring a to ring b is accurately captured supposing that the weld is axisymmetric. The transfer

function from ring b to ring a is further compromised by the presence of the leaked signal coming from the other direction. However, the amplitude of the leaked signal is very small compared to the incident signal in the forward direction. This can be verified by checking the leaked signal in Fig. 2, which is also reflected from the 1st weld but is much smaller than the signal reflected back from the forward incident pulse. The influence of the leaked signal is thus ignored in calculating the transfer functions.

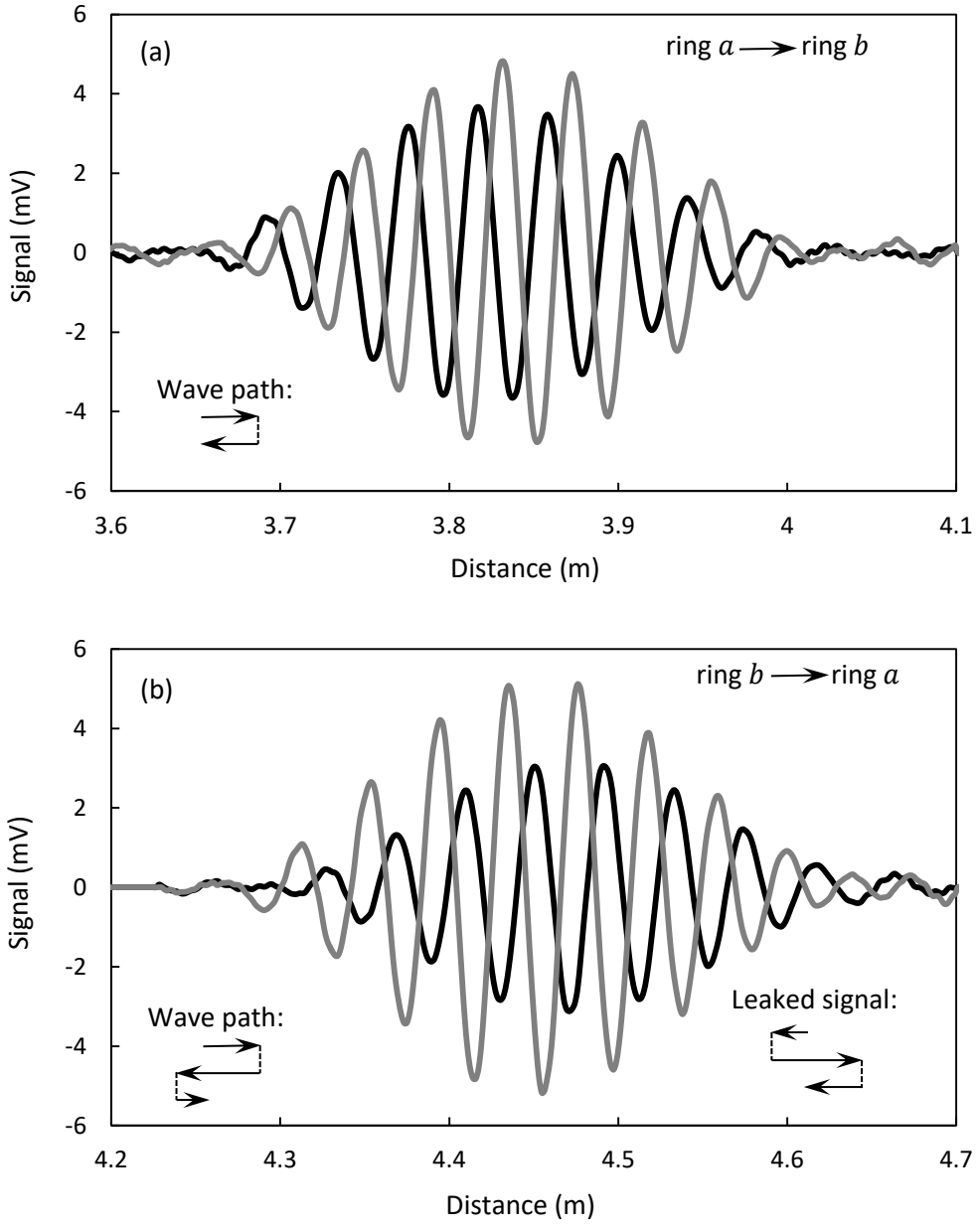

Fig. 5 Reflected pulses for calculating transfer functions between the two rings.(a) wave propagation from ring a to ring b; (b) wave propagation from ring b to ring a. ——, ring a; ——, ring b.

Substitution of the transfer functions into Eq. (1) and the subsequent implementation of the inverse Fourier transform deliver $p_b^-(t)$, i.e., the reflected signal from the forward direction, shown in Fig. 6. Note that a Butterworth bandpass filter has been used to filter the transfer functions. A 10-cycle, Hanning-windowed incident pulse centred at 40kHz is used for Figs. 2 and 6. Based on this, the Butterworth filter has a passband from 30kHz to 50kHz, and a stopband below 10kHz and above 70kHz with an attenuation of 30dB. This eliminates possible noise signature that lies beyond the bandwidth of the incident signal. If the centre frequency of the incident pulse is changed, then the bandwidth of the filter must be changed accordingly. Furthermore, the transducers cannot receive signals when they are transmitting signals, so that there is normally a blind region when the transducers start to produce the 10-cycle, Hanning-windowed incident pulse. To avoid the influence of this blind region, the signal (see Fig. 2) that lies between zero and 2m has been set to zero.

After these procedures, Fig. 6 shows that the number of pulses has been significantly reduced and most of the repeated and leaked pulses have been removed. There is one repeated pulse from the 1st and 2nd weld respectively. The repeated signal from the 2nd weld is larger than the repeated signal from the 1st weld. This is because the repeated signal from the 2nd weld is actually the overlaying of two pulses. The pathway analysis for these pulses is shown in Fig. 7. These pathways all start from the Teletest tool and finish at the tool where the signal is recorded. Each time a pulse is reflected

by a feature, the pathway arrow line in Fig. 7 is moved downwards a little to avoid overlaying the lines. For the repeated signal from the 1st weld, there is only one pathway. However, for the repeated signal from the 2nd weld, two different wave pathways can be identified, and the travel distances of these two pathways are exactly the same. This means that the repeated signal from the 2nd weld represents the overlaying of two pulses and explains why the repeated signal from the 2nd weld is larger than the repeated signal from the 1st weld. A clear space time diagram has been presented by Amir et al [42] which demonstrates how forward and backward waves travel in space and time. Fig. 6 also shows that the reflected signal from the 3rd weld is very small. This is because the 1st and 2nd welds are uncoated, whereas the 3rd weld is coated by Denso Tape. The attenuation ratio is very high in the coated section of the pipe. The length of coating is 4.45m between the tool and the 3rd weld. Following a semi-analytical finite element method derived by Duan et al [41] for coated and buried pipes, the attenuation of T(0,1) is calculated to be 2.8 dB/m at 40kHz for the current Denso Tape coated pipe. This gives a total attenuation of 24.9 dB. The difference between the reflected signal from the 2nd and 3rd welds in Fig. 6 shows an attenuation of 24.3 dB. The numerical and experimental attenuations are thus consistent. This level of attenuation ratio shows the difficulty of using ultrasonic waves to inspect coated pipes. It is relatively straightforward to extract features from pipe sections that are uncoated. However, once the pipe is coated, the reflected signal from the coated section is much reduced and it is necessary to improve signal to noise ratio to identify small features.

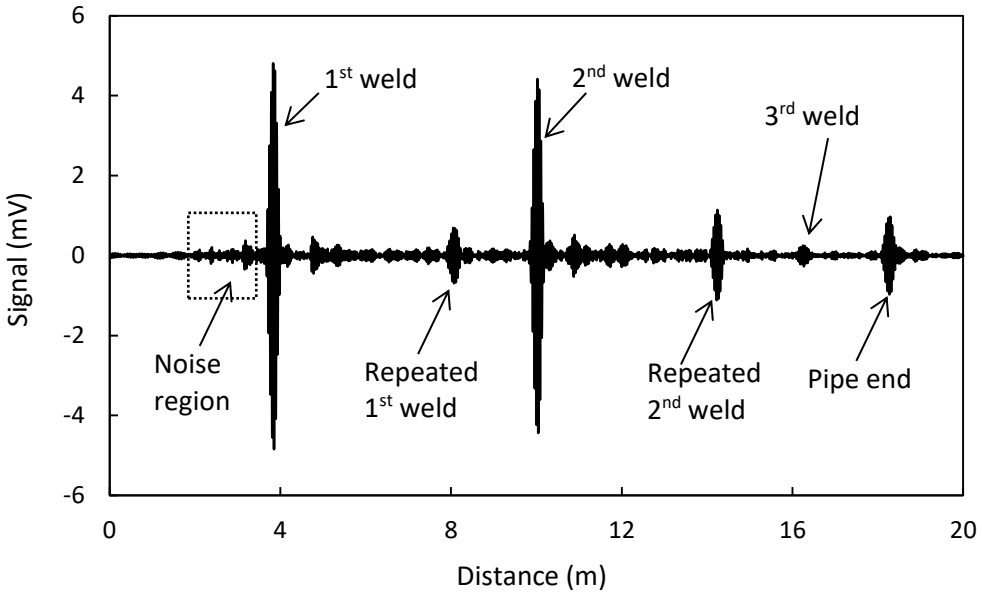

Fig. 6 Reflected signal $p_b^-(t)$ for 40kHz pulse incident on pipe coated with 5.5m Denso Tape.

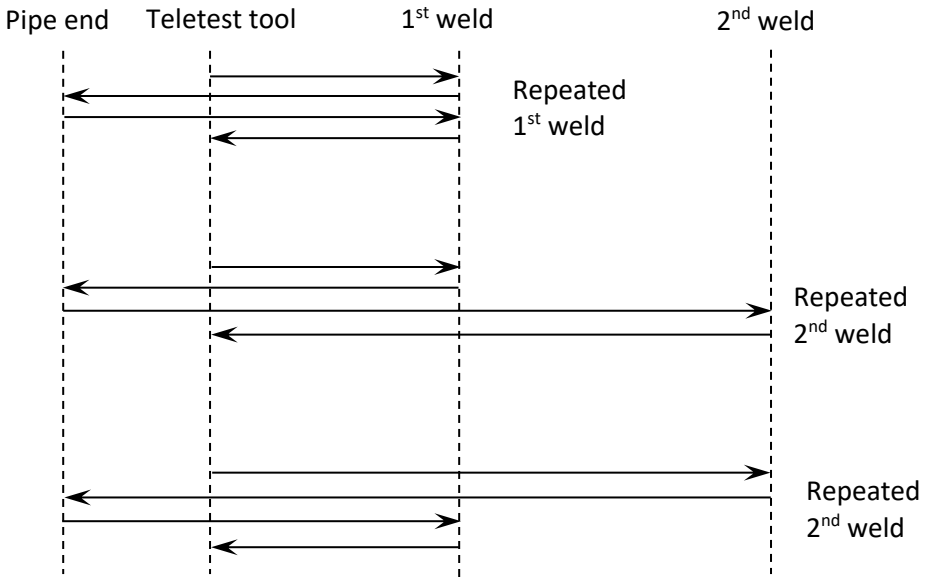

Fig. 7 Wave pathway analysis for repeated pulses associated with the 1st and 2nd weld.

To use the spectral subtraction method, the noise region must be specified so that the noise spectrum $\widetilde{\mathrm{N}}(\omega)$ can be estimated. This requires knowledge of some sections of the pipe or of the signal. In Fig. 6, signal distance between 2m and 3.5m is specified

as the noise region. This is the region between the Teletest tool and the 1st weld. The pipe in this region is uniform without any features, and the noise is coming from piezoelectric, coherent and environmental noise. The noise spectrum $\widetilde{\mathrm{N}}(\omega)$ can be estimated from this region. The segmentation of the signal Eq. (2) requires a Hanning window to be applied to this region. The width of the sliding Hanning window is equivalent to an 8-cycle, Hanning-windowed pulse while the incident signal is a 10-cycle, Hanning-windowed pulse. The amplitude of the first and last cycle is very small and often coloured by noise, so that the sliding window width is set slightly smaller than the width of the incident signal. An 8-cycle window width is used throughout this study. Eqs. (3)-(5) then give the estimated noise spectrum of the signal after an averaging process. This noise spectrum can be removed from the whole signal through the sliding window method. The offset between two adjacent windows is 10% of the window width. Eqs. (6) and (7) deliver the post-processed signal $\tilde{s}(t)$ shown in Fig. 8.

In Fig. 8, the reflected signal from the 1st weld has been normalised, so that the maximum signal amplitude is the same before and after spectral subtraction. The figure is also zoomed-in to show the small peaks close to the noise floor more clearly. The large peaks are of no concern here, because they can be captured and interpreted clearly. It can be seen that the noise floor is significantly reduced after the spectral subtraction, so that the reflected signal from the 3rd weld emerges naturally. The amplitude of the pulse is reduced because of the removal of the noise signature. However, there are a few peaks that have amplitude larger than the amplitude of the reflected signal from the 3rd weld. These peaks could lead to misinterpretation if one is trying to identify small features from these peaks. It is of course possible, and often normal practice, to simply consider all peaks smaller than 10% of the amplitude of a

weld to be noise. This is to say, any signal which has an amplitude that is 20dB smaller than the reflected signal from a weld, could be considered noise. In that case, the 3rd weld would not be identified as a signal, and valuable information is lost.

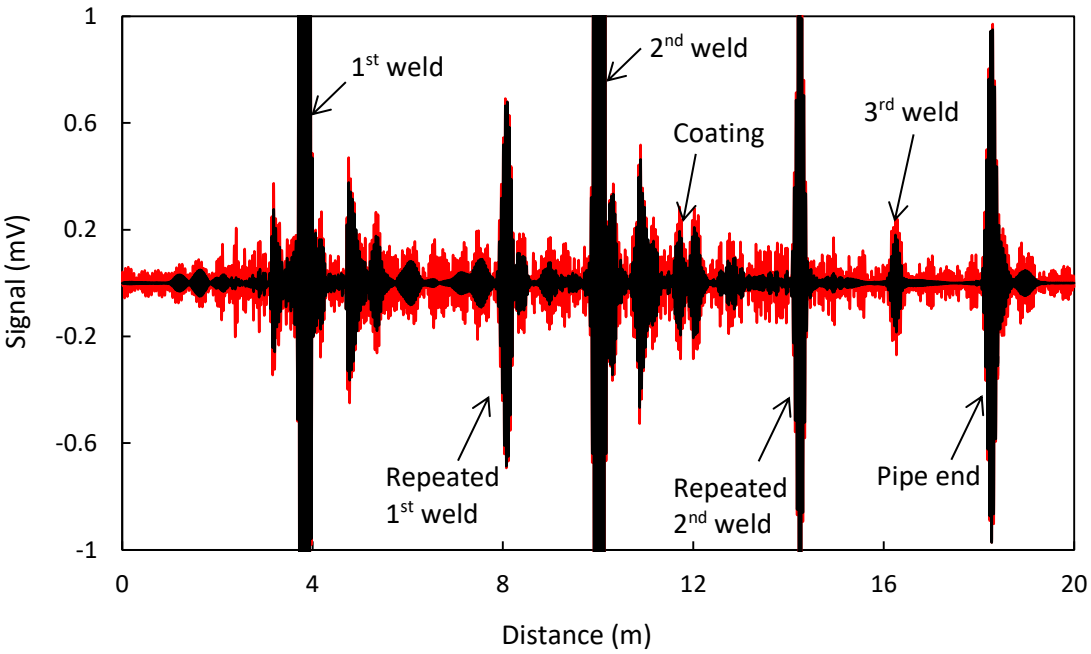

Fig. 8 Reflected signal before and after spectral subtraction for 40kHz pulse incident on pipe coated with 5.5m Denso Tape . ——— , before subtraction, i.e., $p_b^-(t)$; ——— , after subtraction, i.e., $\tilde{s}(t)$.

To further clean up the noise floor, the spectral enhancement method is used on the basis of $\tilde{s}(t)$, shown in Fig. 8. This requires the knowledge of a known signal $T(\omega)$. The reflected signal from the 1st weld is truncated and transformed to the frequency domain, giving $T(\omega)$, and Eq. (8) is then used to determine if a signal is similar to $T(\omega)$ after normalisation. This works because the incident signal is a 10-cycle, Hanning-windowed torsional wave mode, and any scattered signal from narrow axisymmetric features shall also be a 10-cycle, Hanning-windowed torsional wave mode. Thus all the scattered axisymmetric pulses will have almost the same shape, with a difference only in amplitude and arrival time. Note that for relatively large

length axisymmetric features, it might be possible for resonance and anti-resonance frequencies to appear, which is not considered in this paper. The amplitudes of two pulses can be normalised, so that their maximum amplitudes are the same at the centre frequency of the incident pulse (40kHz here). Eq. (8) then determines the similarity of two pulses between the frequency bandwith of 25kHz and 55kHz. After a number of parametric studies, the threshold is set to be 0.2 and any signal with an rms difference less than 0.2 will be considered to be a scattered signal, rather than noise, and will be enhanced. The sliding window technique is used. The window width and the offset value are kept the same.

The post processed signal after spectral enhancement, i.e., $\tilde{z}(t)$, is shown in Fig. 9. The signal is normalised so that the reflected signal from the 1st weld is equal in amplitude before and after spectral enhancement. Because the scattered pulses are enhanced, and the noise is not, the relative difference between scattered pulses and noise will be increased, as shown in Fig. 9. Furthermore, since the width of the sliding window is equivalent to an 8-cycle, Hanning-windowed pulse, and the offset between windows is only 10% of the window width, it is possible to find a small number of windowed pulses that belong to a single 10-cycle, Hanning-windowed pulse. In this case, only the first windowed pulse is enhanced by Eq. (9). The combined effect of spectral subtraction and enhancement is that the noise floor is cleaned up with only a low number of small peaks remaining. This helps to identify any potential signal beneath the noise floor, such as the reflection from the 3rd weld. This is especially important for ultrasonic non-destructive pipe testing under coated or buried conditions, because of the high attenuation of waves propagating in these structures. To clear up the noise floor further, additional work on the classification of signal and noise signatures is required.

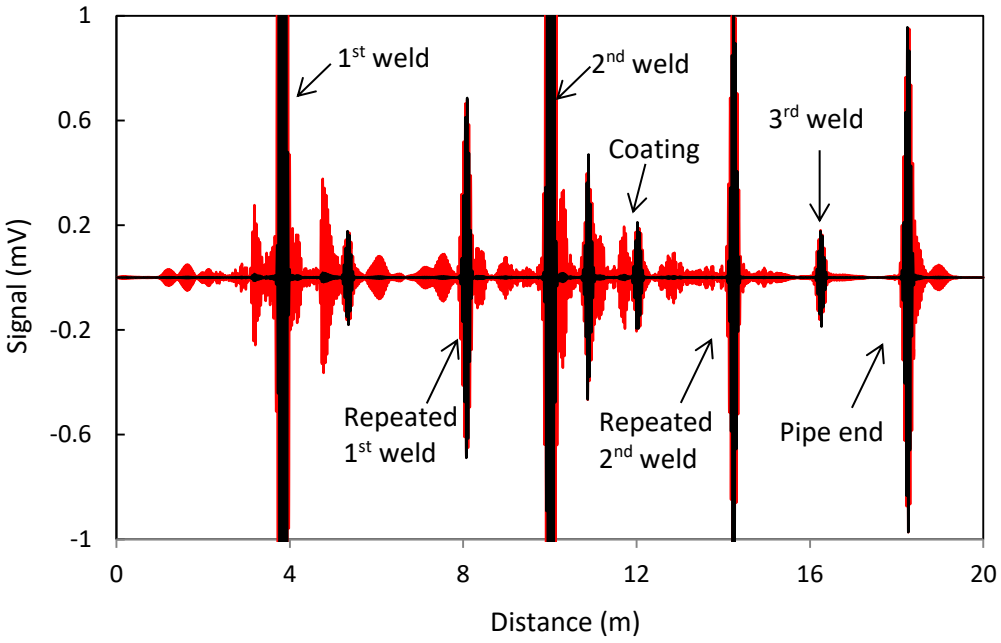

Fig. 9 Reflected signal before and after spectral enhancement for 40kHz pulse incident on pipe coated with 5.5m Denso Tape . ——— , before enhancement, i.e., $\tilde{s}(t)$; ——— , after enhancement, i.e., $\tilde{z}(t)$.

The spectral subtraction and enhancement algorithm has been tested at different frequencies under a number of different test conditions. In Fig. 1, the coating was incrementally wrapped onto the pipe from right to left, allowing measurements to be taken at different coating lengths. For conciseness only some of these results are reported here. Fig. 10 shows the measured signal under a different test condition, where the coating length is 3m, and the incident wave is a 10-cycle, 35kHz centred, Hanning-windowed pulse. Following the same procedure, the backward wave cancelling algorithm based on Eqs. (1) and (2) has been used to cancel waves coming from the backward side of the tool. The signal shown in Fig. 10 is very similar to that shown in Fig. 6. However, the reflection from the 3rd weld and the far pipe end is much stronger in Fig. 10 than in Fig. 6, because of the reduced length of coating. The

length of coating between the 2nd and 3rd weld is 1.95m. The semi-analytical finite element model [41] calculates the attenuation to be 2.8 dB/m at 35kHz for the Denso Tape coated pipe. This gives a total attenuation of 10.9 dB between the 2nd and 3rd weld based on a pulse echo procedure. In Fig. 10, the attenuation between the reflected signal from the 2nd and 3rd weld is measured to be 11.1 dB. The theoretical and experimental attenuations are highly consistent.

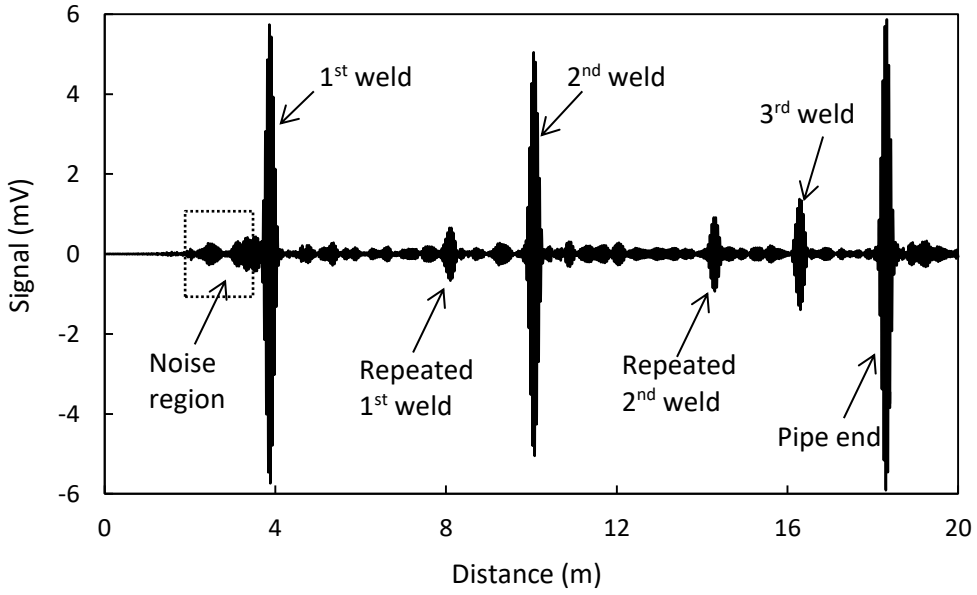

Fig. 10 Reflected signal $p_b^-(t)$ for 35kHz centre frequency pulse incident on pipe coated with 3m Denso Tape.

To clean up the noise floor, the spectral subtraction and enhancement technique is used. The results are shown in Figs. 11 and 12 respectively. The width of the sliding window is equivalent to an 8-cycle, Hanning-windowed pulse, and the offset ratio is 10%. The noise spectrum, $\mathrm{N}(\omega)$ in Eqs. (5) and (6), is calculated based on the signal truncated between the distance of 2m and 3.5m. The signal spectrum, $T(\omega)$ in Eq. (8), is calculated based on the pulse reflected from the 1st weld. The threshold value

d_s is 0.2. It can be seen that the noise signature in Fig. 10 is very different to that shown in Fig. 6. This is because the centre frequency of the pulse is different. Furthermore, the tests were carried out at different times, so that environmental noise is likely to be different and temperature variation could also play a role. However, the algorithm is effective in cleaning up the noise floor under different noise conditions and most of the noise peaks have been removed. A few small noise peaks are still visible which could be removed by reducing the threshold value d_s. However, reducing the threshold value will increase the chance of missing a real signal from a pipe feature as well. It is better to leave a small number of noise peaks in the figure, than accidentally remove a true signal from the measurement. However, the algorithm does significantly improve the ease of discriminating small features from the noise floor, if one is seeking small features under coated or buried conditions.

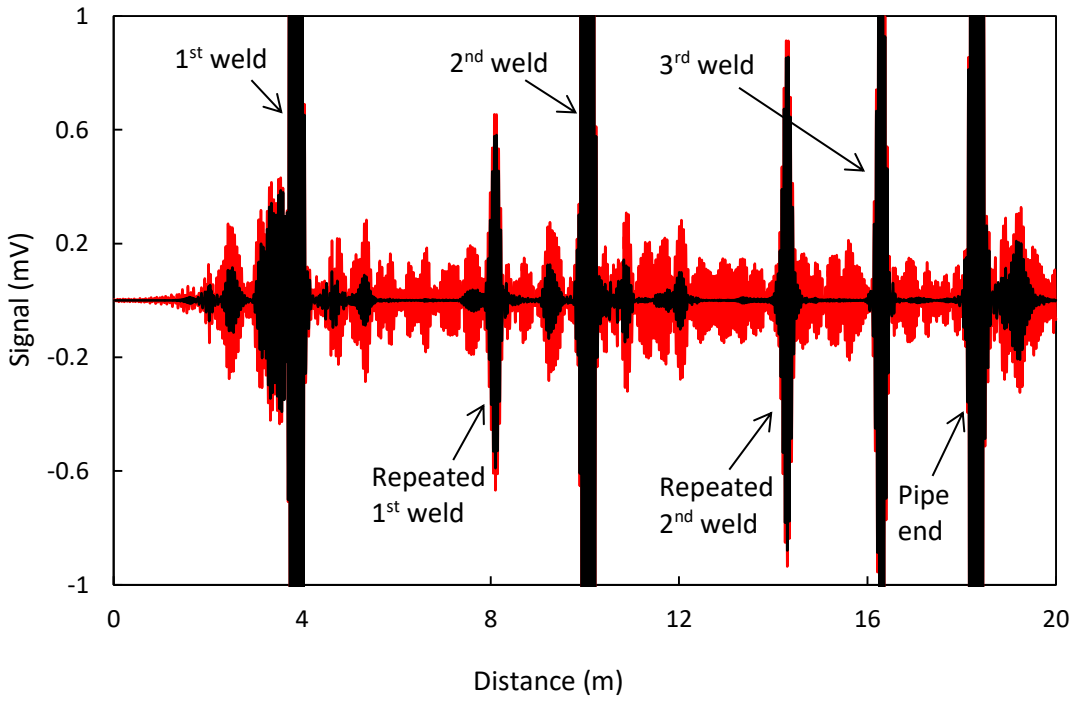

Fig. 11 Reflected signal before and after spectral subtraction for 35kHz pulse incident on pipe coated with 3m Denso Tape. ——— , before subtraction, i.e., $p_b^-(t)$; ——— , after subtraction, i.e., $\tilde{s}(t)$.

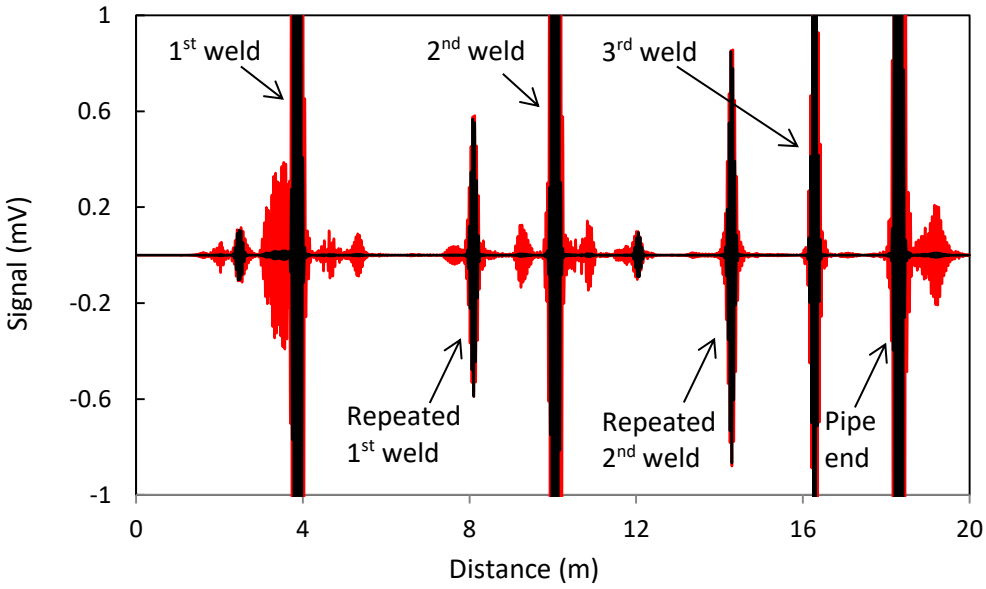

Fig. 12 Reflected signal before and after spectral enhancement for 35kHz pulse incident on pipe coated with 3m Denso Tape . ——— , before enhancement, i.e., $\tilde{s}(t)$; ——— , after enhancement, i.e., $\tilde{z}(t)$.

V. Conclusions

The article investigates signal processing techniques to improve signal to noise ratio associated with torsional wave propagation in Denso Tape coated pipes. The coating

material heavily absorbs sound energy, so that attenuation of the torsional wave is very high. For a coating length that is 5.5m long, the reflected signal from a weld beneath the coating is already lower than the maximum amplitude of the noise peaks. This makes the interpretation of the signal difficult, especially under the coated section. To clean up the signal, a wave separation algorithm is used to remove reflected waves coming from the backward direction along the pipe. This reduces the number of repeated pulses. A spectral subtraction and enhancement technique is then used to improve signal to noise ratio. This requires a noise region to be specified, and a sliding Hanning window is used to divide the noise region into segments. A Fourier transform is applied to each segment, and the noise spectrum is obtained by frequency domain averaging all the segments in the noise region.

Once the averaged noise spectrum is obtained, it can be removed from the total signal using the sliding window technique. The Hanning window is applied to each signal segment. This avoids the discontinuity between adjacent segments. The segments are reconstructed by inverse Fourier transformation, and then combined in the time domain. The noise floor has been significantly cleaned up after this procedure. With this basis, the spectral enhancement technique is applied. A known signal region is specified and the spectrum of this signal is compared to the spectrum of all other segments. If the spectrum of any segment is close to the signal spectrum, i.e., the root mean square difference is small, then the segment is classified as a signal region and the amplitude of this region will be increased by 40dB. This is equivalent to reducing the noise level by 40dB if the amplitude of the signal is normalised to keep the maximum amplitude of the signal the same before and after spectral enhancement. After application of these techniques, most of the noise peaks are removed. The very

few that remain require further work. These noise peaks could possibly be removed by investigating further an algorithm that classifies signal features more accurately and robustly. Further work also involves study of non-axisymmetric defects, and classification and extraction of signatures from non-axisymmetric defects.

Acknowledgements

The authors would like to thank the Innovate UK project (Ultrasonic Nuclear Inspection, Ref. 102077) for supporting the work reported here.

References:

1. Ditri JJ, Rose JL. Excitation of guided elastic wave modes in hollow cylinders by applied surface tractions, J Appl Phys 1992, 72: 2589 - 2597.
2. Rose JL, Ditri JJ, Pilarski A, Rajana K, Carr FT. A guided wave inspection technique for nuclear steam generator tubing, NDT E Int 1994, 27: 307-330
3. Lowe MJS, Alleyne DN, Cawley P, Defect detection in pipes using guided waves, Ultrasonics 1998, 36: 147–154.
4. Demma A, Cawley P, Lowe MJS, Roosenbrand AG, Pavlakovic B, The reflection of guided waves from notches in pipes: a guide for interpreting corrosion measurements, NDT E Int 2004, 37: 167-180.
5. Kirby R, Zlatev Z, Mudge P, On the scattering of torsional elastic waves from axisymmetric defects in coated pipes, J Sound Vib 2012, 331: 3989-4004.
6. Kirby R, Zlatev Z, Mudge P, On the scattering of longitudinal elastic waves from axisymmetric defects in coated pipes, J Sound Vib 2013, 332: 5040-5058.

7. Kuo CW, Suh CS, On the dispersion and attenuation of guided waves in tubular section with multi-layered viscoelastic coating - part I: axial wave propagation, Int J Appl Mechanics 2017, 9: 1750001.
8. Leinov E, Lowe MJS, Cawley P, Investigation of guided wave propagation and attenuation in pipe buried in sand, J Sound Vib 2015, 347: 96-114.
9. Leinov E, Lowe MJS, Cawley P, Ultrasonic isolation of buried pipes, J Sound Vib 2016, 363: 225-239.
10. Duan W, Kirby R, Mudge P, Gan T-H. A one dimensional numerical approach for computing the eigenmodes of elastic waves in buried pipelines, J Sound Vib 2016, 384: 177-193.
11. Long R, Cawley P, Lowe MJS. Acoustic wave propagation in buried iron water pipes. Proc Royal Soc A 2003, 459: 2749-2770.
12. Barshinger N, Rose JL, Guided wave propagation in an elastic hollow cylinder coated with a viscoelastic material, IEEE Trans Ultrason Ferroelectr Freq Control 2004, 51: 1547 - 1556.
13. Mu J, Rose JL, Guided wave propagation and mode differentiation in hollow cylinders with viscoelastic coatings, J Acoust Soc Am 2008, 124: 866 - 874.
14. Castaings M, Lowe M, Finite element model for waves guided along solid systems of arbitrary section coupled to infinite solid media, J Acoust Soc Am 2008, 123: 696 - 708.
15. Hua J, Rose JL, Guided wave inspection penetration power in viscoelastic coated pipes, Insight 2010, 52:195 - 200.
16. Hua J, Mu J, Rose JL. Guided wave propagation in single and double layer hollow cylinders embedded in infinite media, J Acoust Soc Am 2011, 129: 691 - 700.

17. Muggleton JM, Yan J, Wavenumber prediction and measurement of axisymmetric waves in buried fluid-filled pipes: Inclusion of shear coupling at a lubricated pipe/soil interface, J Sound Vib 2013, 332: 1216-1230.
18. Nguyen KL, Treyssède F, Hazard C. Numerical modeling of three-dimensional open elastic waveguides combining semi-analytical finite element and perfectly matched layer methods, J Sound Vib 2015, 344: 158-178.
19. Muggleton JM, Kalkowski M, Gao Y, Rustighi E, A theoretical study of the fundamental torsional wave in buried pipes for pipeline condition assessment and monitoring, J Sound Vib 2016, 374: 155-171.
20. Gao Y, Sui F, Muggleton JM, Yang J. Simplified dispersion relationships for fluid-dominated axisymmetric wave motion in buried fluid-filled pipes. J Sound Vib 2016, 375: 386-402.
21. Benmeddour F, Treyssède F, Laguerre L. Numerical modelling of guided wave interaction with non-axisymmetric cracks in elastic cylinders, Int J Solids Struct 2011, 48: 764–774.
22. Duan W, Kirby R. A numerical model for the scattering of elastic waves from a non-axisymmetric defect in a pipe, Finite Elem Anal Des 2015, 100: 28-40.
23. Duan W, Kirby R. Mudge P. On the scattering of elastic waves from a non-axisymmetric defect in a coated pipe, Ultrasonics 2016, 65: 228-241.
24. Duan W, Kirby R, Mudge P. On the scattering of torsional waves from axisymmetric defects in buried pipelines, J Acoust Soc Am 2017, 141: 3250-3261.
25. Sun F, Sun Z, Chen Q, Murayama R, Nishino H. Mode conversion behavior of guided wave in a pipe inspection system based on a long waveguide, Sensors 2016, 16:1737.

26. Castaings M, Clezio EL, Hosten B. Modal decomposition method for modeling the interaction of Lamb waves with cracks, J Acoust Soc Am 2002, 112: 2567–2582.
27. Vogt T, Lowe M, Cawley P. The scattering of guided waves in partly embedded cylindrical structures, J Acoust Soc Am 2003, 113: 1258-1272.
28. Predoi MV, Castaings M, Moreau L. Influence of material viscoelasticity on the scattering of guided waves by defects, J Acoust Soc Am 2008, 124: 2883-2894.
29. Gravenkamp H, Prager J, Saputra AA, Song C, The simulation of Lamb waves in a cracked plate using the scaled boundary finite element method, J Acoust Soc Am 2012, 132: 1358–1367.
30. Nawaz R, Lawrie JB. Scattering of a fluid-structure coupled wave at a flanged junction between two flexible waveguides, J Acoust Soc Am 2013, 134: 1939-1949.
31. Gravenkamp H. Song C, Birk C. Simulation of elastic guided waves interacting with defects in arbitrarily long structures using the scaled boundary finite element method, J Comput Phys 2015, 295: 438–455.
32. Kemp JA, Walstijn M, Campbell DM, Chick JP, Smith RA. Time domain wave separation using multiple microphones. J Acoust Soc Am 2010, 128: 195-205.
33. Groves KH, Lennox B. Directional wave separation in tubular acoustic systems - The development and evaluation of two industrially applicable techniques, Appl Acoust 2017, 116: 249-259.
34. Boll S. Suppression of acoustic noise in speech using spectral subtraction, IEEE Trans Acoust Speech Signal Process 1979, 27: 113-120.

35. Lim S, Oppenheim AV. Enhancement and bandwidth compression of noisy speech, Proc. IEEE 1979, 67: 1586–1604.
36. Ephraim Y, Malah D. Speech enhancement using a minimum mean-square error short-time spectral amplitude estimator, IEEE Trans Acoust Speech Signal Process 1984, 32: 1109- 1121.
37. Ephraim Y, Trees HL. A signal subspace approach for speech enhancement, IEEE Trans Audio Speech Language Process 1995, 3: 251 –266.
38. Lebart K, Boucher JM, Denbigh PN. A new method based on spectral subtraction for speech dereverberation, Acta Acoustica 2001, 87: 359–366.
39. Li J, Deng L, Gong Y, Haeb-Umbach R. An overview of noise-robust automatic speech recognition, IEEE Trans Audio Speech Language Process 2014, 22: 745-777.
40. Upadhyay N, Karmakar A. Speech enhancement using spectral subtraction-type algorithms: a comparison and simulation study, Procedia Comput Sci 2015, 54: 574 - 584.
41. Duan W, Deere M, Mudge P, Kanfoud J, Gan T-H. Modelling and measurement of guided wave propagation in Denso Tape coated pipes, First World Congress on Condition Monitoring, London, UK, 2017
42. Amir N, Shimony U, Rosenhouse G, A discrete model for tubular acoustic systems with varying cross section - the direct and inverse problems. Part 1: Theory, Acta Acust. United. Ac. 1995, 81: 450-462.